UNIVERSITY OF CALIFORNIA SAN DIEGO

Characterization of MBOAT7 knockout in mice and human cells

A thesis submitted in partial satisfaction of the requirements for the degree Master of Science

in

Biology

by

Isaac Tang

Committee in charge:

Professor Joseph Gleeson, Chair
Professor Amy Kiger, Co-chair
Professor Susan Ackerman

2021

The thesis of Isaac Tang is approved, and it is acceptable in quality and form for publication on microfilm and electronically.

University of California San Diego

2021

TABLE OF CONTENTS

ACKNOWLEDGEMENTS

I would like to thank Dr. Joseph Gleeson for his role as the chair of my committee as well as the invaluable guidance provided throughout the duration of the construction of this thesis. I would also like to thank Dr. Amy Kiger and Dr. Susan Ackerman for serving as my co-chair and committee member respectively.

I would like to acknowledge the members of the Gleeson Lab, especially Swappi Mittal for aiding me not only in certain experiments in the project, but also in guiding and teaching the concepts involved. I would also like to thank Anide Johanssen, who generated the conditional knockout mice shown in Figure 4.

I would also like to thank Dr. Ben Cravatt and specifically Alex Reed for his excellent work on the lipidomics involved in this project.

ABSTRACT OF THE THESIS

Characterization of MBOAT7 in mice and human cells

by

Isaac Tang

Master of Science in Biology

University of California San Diego, 2021

Professor Joseph Gleeson, Chair
Professor Amy Kiger, Co-Chair

The loss of the gene membrane-bound O-acyltransferase 7 (*MBOAT7*) is associated with intellectual disability, seizures, and autism-like features in humans [OMIM 606048]. *MBOAT7* codes for the protein lysophosphatidylinositol acyltransferase 1 (LPIAT1), which preferentially esterifies arachidonoyl-CoA to the Sn2 position of lysophosphatidylinositol, generating the predominant 20:4 containing species of phosphatidylinositol. Here we show that the knockout of *Mboat7* causes spatially and temporally restricted cell death in the embryonic murine neocortex, leading to disrupted radial glia patterning and diminished cortical thickness. We also show a significantly altered lipidome in both *Mboat7* knockout mice and human neural tissue, as well as a dynamic equilibrium of lipid species in differentiating patient derived neural progenitor cells.

We hypothesize that these characteristics contribute to the encephalopathies of *MBOAT7* patients.

Introduction

Lipids, often characterized by their hydrophobicity, describe a class of biomolecules that are often grouped into three main categories: fatty acids, phospholipids, and sterols [1]. Phospholipids, perhaps the least studied of the three, are generally known for their polarity and their role in constructing the phospholipid bilayer in cell membranes. These molecules generally consist of two fatty acids esterified to a glycerol backbone, which is in turn attached to a polar headgroup. Phospholipids are separated into different classes based on the head groups attached to the glycerol, such as: phosphatidylethanolamine (PE), phosphatidylcholine (PC), phosphatidylserine (PS), and the subject of this paper and the most negatively charged of all the headgroups, phosphatidylinositol (PI).

PI is generated primarily via two mechanisms, the first involving de novo synthesis with the combination of cytidine diphosphate diacylglycerol (CDP-DAG) and inositol via phosphatidylinositol synthase, and the second involving the remodeling of lysophosphatidylinositol via the Land's cycle [2]. The subject of this thesis focuses specifically on the actions of the gene membrane-bound O-acyltransferase 7 (*MBOAT7*) and the protein it codes for, lysophosphatidylinositol acyltransferase1 (LPIAT1), which is involved in the latter of these synthetic mechanisms. LPIAT1 selectively esterifies arachidonoyl-CoA onto the Sn2 position of lysophosphatidylinositol forming the 20:4 species of PI, which is the predominant species of PI in mammalian cells [3].

PI can be further phosphorylated at different sites in either the 3, 4, or 5 position (PIP), after which it can be phosphorylated again up to two more times, until each of the three positions are filled. These different PIP species serve as intracellular regulators of the endocytic pathway, with the different subspecies of PIPs acting as 'barcodes' or as second messengers activating

downstream molecular pathways. For instance, PI(3)P is found predominantly on early endosomes and autophagosomes, PI(4)P on the trans Golgi network, PI(3,5)P2 on sorting endosomes, and PI(3,5)P2 on late endosomes [4]. This selectivity allows the cell to uniquely detect and identify the specific liposome compartment and its function, a feature essential for efficient trafficking.

The fatty acid chains constituting the PI species may also serve to regulate function, with different lengths and unsaturations corresponding to different physical properties of the membrane. Though little is known about the specific nuances of these characteristics in PI, it is thought that the secondary structures formed with the different unsaturations may lead to differences in cell membrane fluidity and different protein binding properties [5]. In addition, downstream PI species can also serve as second messengers themselves, with perhaps the best known being the role PI(4,5)P2 plays in in the $G_{i/o}$-transduction pathway, being converted into inositol triphosphate (IP3) and diacylglycerol (DAG) by the phospholipase C family [6]. This ultimately activates phosphokinase C (PKC) and serves to regulate the concentration of intracellular calcium, leading to mediation of multiple downstream activation pathways. Another well-known second messenger is PI(3,4,5)P3 and the role it plays in the PI3K/AKT/mTOR pathway in cell cycle regulation. Thus, although the molecular interactions of different PI species are varied and deeply interconnected with multiple cell signalling pathways, the specific mechanisms behind these interactions are poorly understood. DAG itself can be reversibly hydrolyzed or esterified into monoacylglycerols (MAGs) and triacylglycerols (TAGs, or simply triglycerides), respectively. One of the more infamous MAGs, 2-arachidonoylglycerol (2-AG), is one of the brain's main endocannabinoids, and are synthesized from the 20:4 (arachidonoyl) containing species of DAG, thereby implicating *MBOAT7* as potentially playing a crucial role in

endocannabinoid signalling. In addition, DAG can react with CDP via CDP-DAG synthase to form the CDP-DAG, which can then be used in the de novo synthetic pathway of PI (Figure 1).

MBOAT7 has previously been implicated as a potential source of pathogenicity in both the liver and the brain. In the liver, *MBOAT7* expression is negatively correlated with body fat mass, where common single nucleotide polymorphisms (SNPs) correlate with hepatic steatosis and is a risk factor for non-alcoholic fatty liver disease (NAFLD) [7]. The same study found that in the mouse liver, *Mboat7* downregulation is associated with increased transcription of pro-inflammatory and pro-fibrotic genes, as well as increased susceptibility for insulin resistance. In addition, hepatic sections of *Mboat7* KO mice show enlarged lipid droplets, a phenomenon that is supported by the overall increase in TAG levels in the liver. Previously, our lab identified six consanguineous families with biallelic inactivating mutations within *MBOAT7* that produced 16 patients with moderate to severe intellectual disability, epilepsy, and autistic features. A previous publication on *Mboat7* knockout mice showed cortical cell death, dysregulated cortical lamination, decreased cortical thickness, and lowered mendelian ratios as well as postnatal lethality [8]. However, the mechanism connecting lipid profile dysregulation to corticogenesis and neural apoptosis is still unclear.

Methods

Prior to starting this master's project, the following reagents had already been established in the lab, and was used for subsequent experiments:

- Straight knockout and conditional *Mboat7* knockout mice
- iPSC derived NPCs from *MBOAT7* patients and family-member controls.

Cell Culture

Neural progenitor cells differentiated from induced pluripotent stem cells (iPSCs) were maintained in DMEM:F12 supplemented with 1X Glutamax (Gibco, 10565018), 1X B27 supplement (Gibco, 0080085SA), 1X Non-essential Amino Acids (Gibco, 11140050), 1X N2 supplement (Gibco, 16502048), and 40 ng/uL FGF2 on poly-L-ornithine / Laminin coated plates. Media changed every other day. For week 1 differentiation, B27 supplement was switched to the without Vitamin A variant and FGF2 was removed. For the following weeks of differentiation, 50% Neurobasal medium was added to week 1 differentiation medium.

Cryosectioning

Pregnant dams were sacrificed at selected time points and embryos harvested in ice-cold PBS. The tails were dissolved in an alkaline lysis buffer and genotyped using primers outlined in Lee et al (2012). The embryo heads were then fixed overnight in 4% PFA at 4°C. The following day, the brains were dehydrated in 30% sucrose. After the brains had sunk to the bottom of the sucrose solution, they were embedded in Negative 50 and placed in -80 degrees for storage. Embedded brains were allowed to equilibrate in the cryostat for 1 hour before sectioning, after

which sections at a thickness of 14 μm. The sections were collected on microscope slides and were allowed to dry at room temperature overnight.

Immunofluorescence

Mounted sections were washed 3 times for 5 minutes each wash with PBS and placed in a steamer for 25 minutes in antigen retrieval solution. The slides were then washed again in PBS 3 times for 5 minutes. They were then permeabilized in PBST (PBS + 0.3% TritonX-100) for 10 minutes and incubated in blocking buffer (5% Donkey Serum in PBST) for 1 hour before overnight incubation with the primary antibody in blocking buffer overnight at 4°C. The slides were then washed 4 times in PBST for 10 minutes and the secondary antibody was added. The slides were incubated for 1 hour at room temperature in the dark. DAPI solution (1 ug/mL) was then added to the slides and allowed to incubate for 15 minutes. The slides were then washed again 4 times for 10 minutes in PBST. The slides were then mounted with Fluoromount-G and allowed to cure overnight before imaging. Ctip2 and Cux1 positive cell quantification was done in a double blinded manner.

Antibodies

Primary: Abcam Cleaved Caspase 3 (ab3623, 1:300), Biolegend TUJ1 (801211, 1:1000), Santa Cruz Doublecortin C-18 (sc8066, 1:300), Abcam TBR2 (ab23345, 1:500), Abcam TBR1 (ab31940, 1:500), BD Biosciences SOX2 (MAB2018, 1:200)

Nile Red Staining

Nile red was diluted in DMSO to a stock concentration of 30 mM. This solution was then diluted 1:3000 and incubated in live cells as well as mounted sections (+DAPI) for 15 minutes. The green (GFP, 488) channel was used to detect the presence of lipid droplets.

Lipidomics

Cells and tissue were lysed in a chloroform:methanol (2:1) solution spiked with internal lipid standards, and then vortexed for 30 seconds and centrifuged at 1400g for 3 minutes at 4°C. The organic layer was harvested and the remaining aqueous layer was subjected at acid extraction (addition of same chloroform:methanol solution + 3N HCl) and vortexed for 30 seconds, after which the solution was centrifuged again and the organic layer was once again collected. The solution was then dried with an N2 stream. The extracted lipids were resuspended in 150 uL of chloroform methanol solution and then injected into the liquid chromatography-mass spectrometer (20 uL for DAG/MAG and 7.5 uL for free fatty acids). All measurements were normalized to the protein concentration as measured with BCA quantification.

Statistics

All statistics were done in the Python Scipy package. Normality was assessed through normaltest, a function based on D'Agostino's and Pearson's test. Significance was determined using the Student's T-test and corrected for multiple comparisons. Fold change (FC) across differentiation was done using week 4 compared to week 0 samples.

Results

Mouse Results

Although previously reported that cell death in embryonic *Mboat7* KO mice brains, the specific time points at which this cell death occurred was not known. We determined that apoptosis, as measured by cleaved caspase 3 positive cells, peaked in the *Mboat7* knockout (KO) murine neocortex at around E14.5, and diminished rapidly thereafter. No significant apoptosis over the background was detected in the heterozygous (HET) mice. This allowed us to narrow both the spatial as well as temporal window of the apoptosis, pointing to a specific time during neuronal development that rendered the cells vulnerable. The cell death appeared to be occurring mainly in the cortical intermediate zone, with less cell death occurring in the ventricular zone (Figure 2).

To determine the specific type of cells dying during brain development, crossed mice with floxed *Mboat7* exon 5 with Cre recombinase driven by four different promoters, which were compared to the straight knockout. These promoters were cell-specific for astrocytes (GFAP), microglia (Cx3cr1), neurons (Synapsin), and neural progenitors (Nestin). The brains were then harvested at E18.5, fixed, embedded, sectioned, and stained for Cux1 (superficial layer) and Ctip2 (deep layer) cortical markers. We found that at E18.5, there were significantly fewer Cux1 positive cells in the Nestin-Cre mice as well as in the straight knockouts at time point E18.5 (Figure 3) ($n > 5$, $p < 0.05$). This was particularly interesting, as Cux1 is a marker for upper layer neurons that are typically born around E13.5, which is when the apoptosis was noted. Cux1 and Ctip2 positive cells normally form distinct upper and lower layers, respectively. In the knockout mice however, we found that the Cux1 positive neurons were expressed in the same layer as the Ctip2 positive neurons, suggesting migratory defects.

Combined with the previous information, we next examined the different progenitor cell populations at the time of cell death. We hypothesized that the ventricular-zone localized Sox2 expression would be relatively similar between the KO and HET mice, since there was little cell death in the ventricular zone, but more substantial cell death in the intermediate and marginal zones. This, along with the knowledge that the phenotype was stronger in immature cell types, led us to believe that much of the cell death that was occurring was in intermediate (basal) progenitors. Thus, we harvested and sectioned *Mboat7* knockout and heterozygous mice at timepoints E12.5 (before apoptosis), E14.5 (peak apoptosis), and E16.5 (after apoptosis), and stained the brain with factors expressed sequentially by radial glia: Sox2 for the apical progenitors, Tbr2 for basal progenitors, and Tbr1 for postmitotic neurons. As predicted, Sox2 expression remained similar across all conditions, but the Tbr2+ cell population in the KO mice at E14.5 and E16.5 was sparser than in the HET condition (Figure 4). This corresponded to a subsequent scattering of Tbr1 positive cells at E16.5 in the KO condition compared to the HETs, forming a pattern consistent with either the overmigration of the cells towards the marginal zone, or a general loss of the upper cortical layers.

Patient NPC

We next asked if there were any significant differences in the lipidome of the developing brain associated with *MBOAT7* knockout. We decided to look at all the metabolites in the Lands cycle pathway, beginning with LPI species, PI species, DAG species, and finally MAG species. We predicted that 20:4 PI species would be decreased as it is the molecule directly downstream of *MBOAT7*, and LPI species to be increased. To do this, we analyzed mouse E13.5 brains (Figure 5) and human NPCs (Figure 6) differentiated from iPSCs reprogrammed from patient

fibroblasts containing a patient-derived in-frame deletion in *MBOAT7* exon 6 (c.758_778del [p.Gln253_Ala259del]). Analysis was in collaboration with the Cravatt Lab at Scripps Research Institute for lipid extraction and mass spectroscopy. As expected most, though not all, 20:4 containing species of PI were diminished in the KO cells and brains compared to the HETs, with significant reduction in the two largest PI species, 18:0/20:4 (FC: Mouse = 0.69, NPCs = 0.18) and 18:1/20:4 (FC: Mouse = 0.42, NPCs = 0.27) ($n = 4$, $p < 0.05$). In addition, non-20:4 containing PI species show a drastic increase in KOs compared to HETs, such as 16:0/18:1 (FC: Mouse = 4.72, NPC = 7.11) and 18:1/18:1 (FC: Mouse = 4.72, NPC = 6.96) ($n = 4$, $p < 0.05$), a phenotype which was previously reported in the postnatal mouse brain and liver. This disparity carried over to downstream DAG, which showed a similar increase in non-20:4 containing species and a decrease in 20:4 containing species, though to a lesser degree than PI. Despite these increases, the total amount of PI was still decreased in the mouse. In the NPCs, the loss of the predominant 20:4 PI species appears to have been largely compensated for by the 18:1/18:1 species, which is not *MBOAT7*-dependent synthesis. In addition, the total amount of DAG appears to be elevated in the HET condition compared to the KO condition, which was the opposite of what was seen in the mice. This data suggests that the loss of *MBOAT7* leads to a major reduction in 20:4 PI species which, being the predominant PI species, leads to a diminishment of overall PI species.

We next assessed if there was a change in a particular lipid species through differentiation that could explain apoptosis seen in the mouse. Patient NPCs were differentiated for 4 weeks, with samples being taken every week for lipidomic analysis. As the cells differentiated, there was a general increase in total PI in both the HET (FC: 1.97) and KO (FC: 1.60), but in all conditions there was less 20:4-containing PI than in the HET conditions (Figure

7) ($n = 3$, $p < 0.05$). In contrast, although there was a slight increase in total DAG in the HET condition (FC: 0.28), there was a significant decrease in the KO cells (FC: 0.48) ($n = 3$, $p < 0.05$). A deeper look into the individual species of both PIs and DAGs revealed a more nuanced lipid profile: For PI, the 20:4 containing PI species in the KOs tended to remain less than their HET counterparts with some, such as 18:0/20:4 even partially making up the difference as differentiation occurred (FC: from 0.18 to 0.45) ($n = 3$, $p < 0.05$). However, some species, notably the 16:0/16:0 containing species, increased the difference between the KO and HET conditions as differentiation progressed (FC: 1.78 to 2.46) ($n = 3$, $p < 0.05$). Interestingly, only the 18:1/18:1 species of PI decreased significantly over the course of differentiation, which is the very species that was the most compensatory in the NPCs (FC: KO = 0.52, HET = 0.59) ($n = 3$, $p < 0.05$). In DAGs, only two species significantly decrease in the HET: 18:1/18:1 (FC: 0.53) and 16:0/18:1 (FC: 0.56), but five species significantly decrease in the KO: 18:1/18:1 (FC: 0.19), 16:0/18:1 (FC: 0.24), 18:1/18:0 (FC: 0.37), 16:0/16:0 (FC: 0.68), and 16:0/18:0 (FC: 0.57) ($n = 3$, $p < 0.05$). In general, LPIs increased over the course of differentiation, although large variances make this generalization tenuous. MAGs largely followed the trend of PI, in which differentiation led to a gradual increase, with slight differences between KO and HET cells (FC: ~2 for all species) ($n = 3$, $p < 0.05$). The exception to this was 20:4 MAG, better known as 2-AG, the levels of which formed an inverted U, peaking at around week 2 and diminishing thereafter. This data suggests that although PI species are increasing in both HET and KO, in the KO cells this increase is coming at the cost of downstream DAG signaling. It also implicates 18:1 containing species as these tended to counter the trend by decreasing in species over the course of differentiation.

Discussion

Our studies point to an essential role that the cellular lipid profile plays in neuronal development. As of now it is still not known whether the alterations seen in the lipidomics are sufficient to lead to the phenotype in humans and mice, nor is it known which species is playing the causative role in the induction of apoptosis. However, there are several theories. The first points towards the insufficiency of certain lipid species that leads to cell death, namely the absence of catalytic *MBOAT7* activity leads to a lack of a 20:4 containing molecule, such as PI or DAG. Considering the predominance of 20:4 PI, the former species would be the most likely culprit. If this is the case, then the exogenous addition of these species may allow the rescue of the phenotype seen in both humans and mice. The compensatory mechanism shown by the spike in other, non 20:4 containing PIs and DAGs leads us to the next hypothesis, which is that a non 20:4 species of PI or DAG that is attempting to make up the deficit is toxic to the cell, and its accumulation is triggering apoptosis. If this is true, then the exogenous addition of the toxic lipid species may exacerbate the condition. A possible candidate for these species can be found in the significant elevation of 18:1/18:1 containing species of both PI and DAG, which noticeably countered the trend by rapidly diminishing throughout differentiation, as well as being the most compensatory of all the PI species in the human NPCs. As synthesis of 18:1/18:1 PI is not *MBOAT7* dependent, it is possible the increase in this species is capable of alleviating the loss of 20:4 containing PI. Unfortunately, the protein that esterifies 18:1 PI into lyso-PI is not known. Interestingly, 18:1 is also known as oleic acid, a fatty acid that is often used to stimulate lipid droplets in culture [10]. Increased lipid droplet size has previously been found as a biomarker of fatty liver disease and lipid droplet accumulation found in *Mboat7* KO E15.5 brains stained with Nile red (data not shown). A third hypothesis is that a deficit of arachidonate containing 2-AG

leads to a lack of signalling via the endocannabinoid system, knockout of which has been implicated in neurodevelopmental problems [11]. However, the 2-AG levels seemed to be only slightly, though significantly, decreased. In all of these cases, the specific mechanism of how lipid dysregulation leads to any of the signalling pathways that might induce apoptosis are unclear. However, the time point at which the cell death is occurring is telling, as E13.5 in the mouse cortex is implicated as a time where preplate splitting occurs, a process essential to the formation of the upper cortical layers. In addition, it was found that 88% of non-syndromic intellectual disability genes are upregulated at this time [9]. Indeed, one of the genes implicated at this time point is ACSL4, a gene that encodes the protein responsible for adding coenzyme A to arachidonic acid. Therefore, cell death at this stage plays a likely candidate of the decreased cortical thickness in mice as well as the intellectual disability seen in humans.

One of the enduring problems we faced was our inability to see the kind of cell death that was seen in mice in the human NPCs. There are several possible reasons for this apparent discrepancy. It could be possible that there is something in the media that rescues the kind of cell death that is not present in the mouse brain. For instance, in vitro culture most lipids are added in the form of supplemental fatty acids or serum, or are synthesized de novo. In contrast, lipids in vivo are usually complexed to different lipoproteins in the blood, forming micelles that carry these hydrophobic species, allowing them to better dissolve. For this reason, the fatty acid composition is generally not as varied in culture as the species that are exposed to the brain in vivo. Alternatively, it could be that there is something in the mouse brain that is triggering cell death that is not present in culture. As mentioned before, E13.5 in the mouse brain is a time in which many developmental processes are beginning to occur. Apoptosis in the mouse cortex could be a result of activation of migratory and differentiation pathways by reelin or signalling

molecule gradients, or could be dependent on structural distribution of specific cell types. Finally, it could simply be that the NPCs are not a very good vector of study for recapitulating the phenotype. Perhaps we simply have not differentiated the cells far enough to mimic the cell distribution in vivo, there are compensatory mechanisms in human cells that are not present in the mice, or we have incorrectly assumed that the same cell death that occurs in the mice occurs in humans. This last possibility seems unlikely, however, as the similarity between the lipidomics data suggests there is at least some overlap in the flux of PI species between the two vectors of study. Regardless, a lack of a clear cell death phenotype in the NPCs makes it difficult to test the kind of biochemical manipulation mentioned in the previous section. Thus, any future steps should be aimed towards finding the right stressor that might elucidate the phenotype in vitro.

Although specific fatty acid species, such as docosahexaenoic acid (DHA), are known to have unique and beneficial effects in terms of cardiovascular and brain health, our study points to a preservation of carbon composition specific processes beyond the free fatty acid stage. The overall increase in most species during differentiation is not altogether surprising, considering as the cells differentiate they extend processes that increase the surface to volume ratio. Because the lipids are normalized by protein concentration, it makes sense that the extension of these lipid bilayer coated processes would outpace the contents of the cell, thereby increasing the ratio of lipid to protein. As *MBOAT7* is knocked out, it might be surprising to see any increase in 20:4 PI species during differentiation, though this could be explained by either 20:4 PA or DAG being converted back into PI via the de novo pathway. Thus, it is worthwhile to see if the knockdown of the gene CDIPT, which codes for PI synthase, would lead to preferential cell death in KO versus HET cells. Unique fluxes in the different PIs and DAGs throughout differentiation hint at

currently unknown mechanisms regulating the buildup and breakdown of each species. For instance, the 16:0 containing species of PI in the KOs rapidly outpaces the levels seen in the HETs throughout differentiation, accompanied by a decrease in their complementary species of DAG. As there were unique fatty acid species of DAG that are increasing and decreasing during differentiation, this could account for the rapid depletion of total DAG levels throughout differentiation. This interaction possibly implicates 16:0 containing PI accumulation or the subsequent depletion of DAG as a source of apoptosis, but also points towards much more nuanced roles of individual fatty acid composition in compound lipid species.

In this study, we have examined the different effects of the loss of *MBOAT7* in both mouse and human neural cells. We have seen significant alterations between heterozygous and knockout conditions in both the cellular distribution as well as the lipidomic profile in neuronal developing cells. Although the mechanism is still unclear, we believe that these differences contribute toward the development of intellectual disability and autistic features seen in human children.

APPENDIX

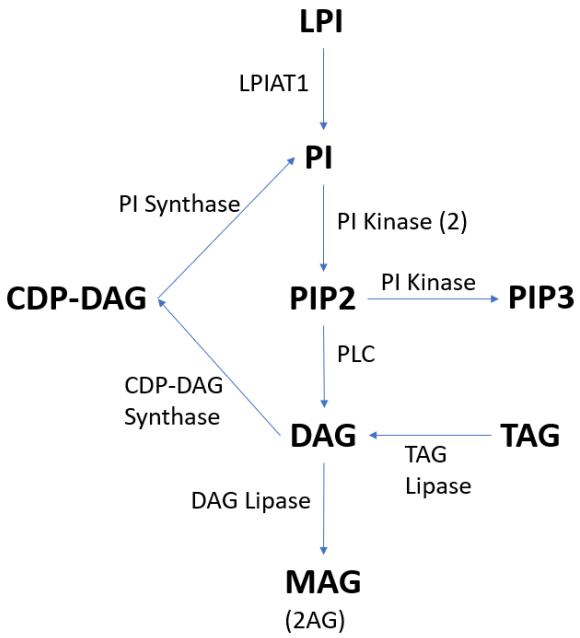

Figure 1: The MBOAT7 Pathway
In mammals, AA is added to LPI by MBOAT7(LPIAT1) to form 20:4 containing PI. PI is then reversibly phosphorylated twice through various PI kinases to make PIP2, which can then be phosphorylated again to make PIP3, or hydrolyzed to form IP3 and DAG by PLC. DAG can then be reversibly converted to MAG, TAG, or CDP-DAG by DAG lipase, TAG lipase, or CDP-DAG synthase, respectively.

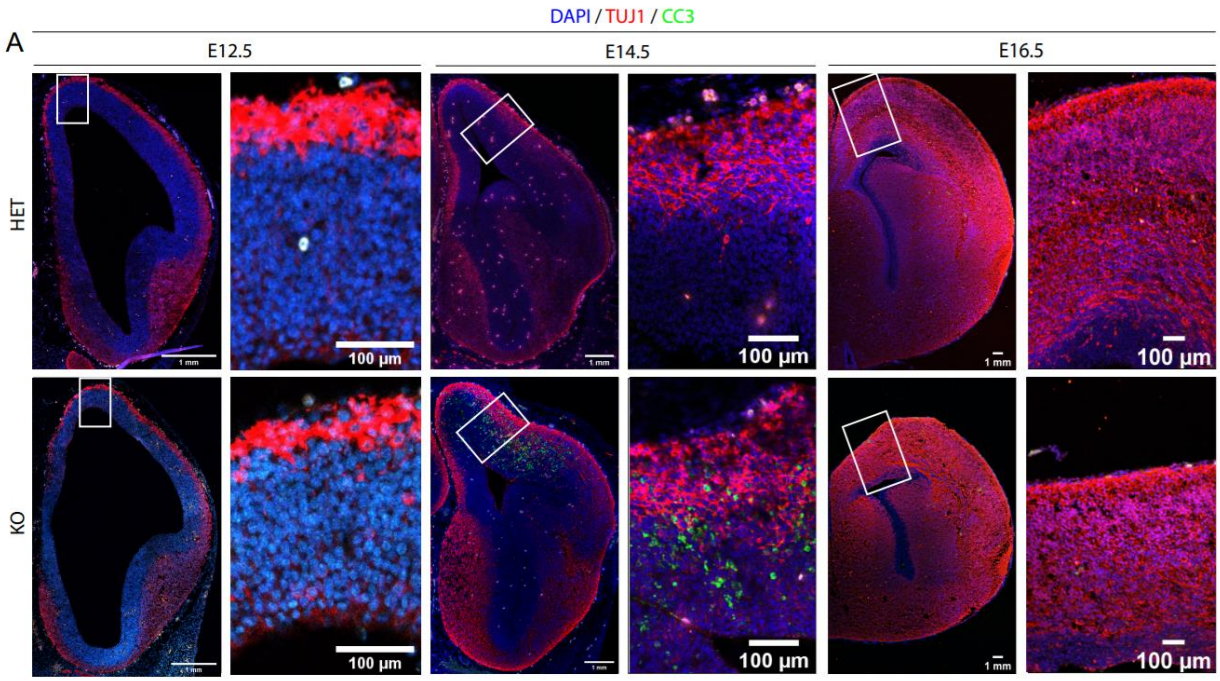

Figure 2: Apoptosis in the murine cortex is spatially and temporally restricted
A) Cell apoptosis as marked by cleaved caspase 3 activity is located throughout the MBOAT7 homozygous knockout mouse neocortex compared to the heterozygous knockout, and is present at E14.5, but not E12.5 or E16.5.

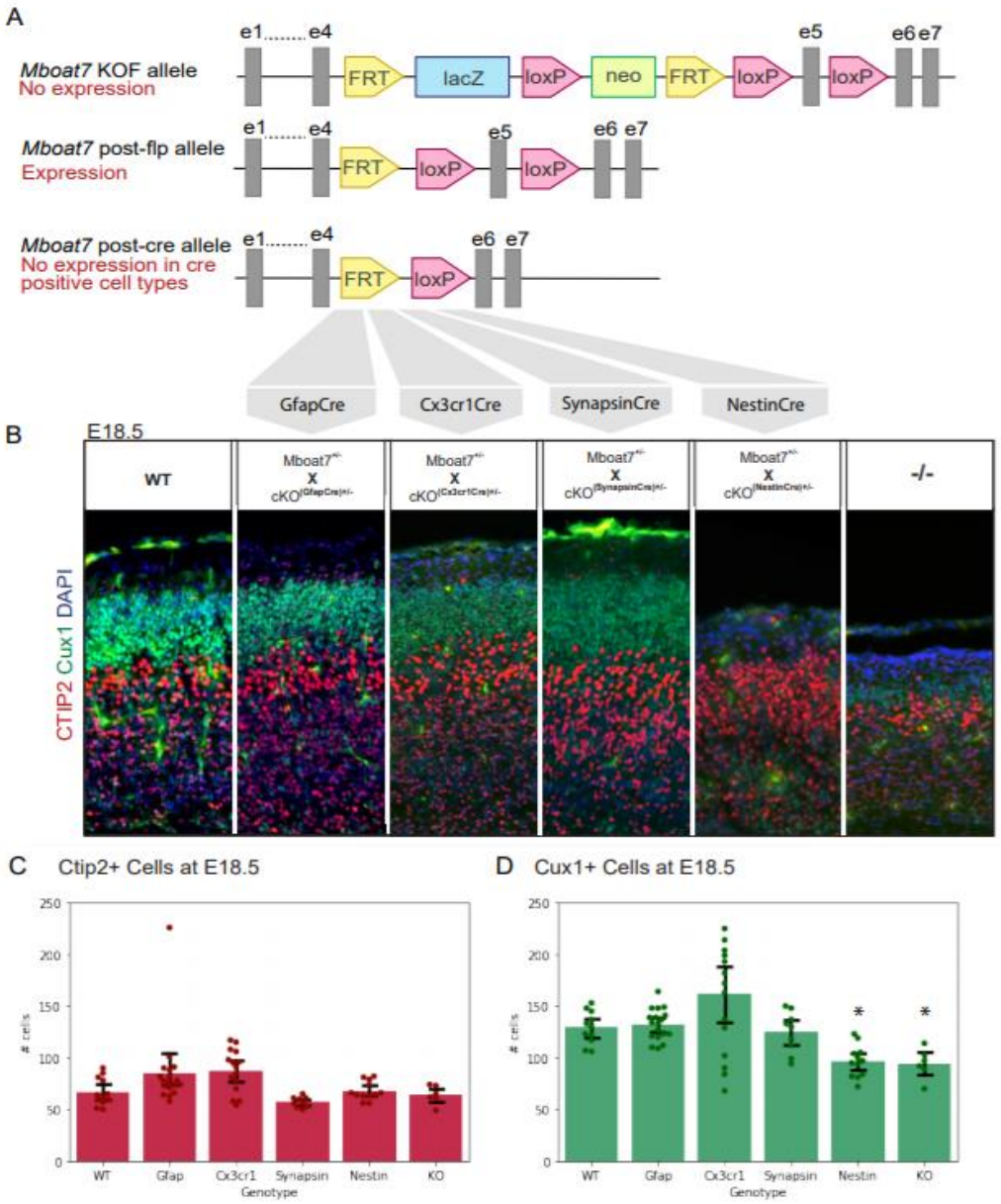

Figure 3: MBOAT7 KO in progenitor cells leads to cortical lamination phenotype
A) Conditional knockout construct of MBOAT7 with Gfap (astrocytes), Cx3cr1 (microglia), synapsin (neurons), and Nestin (neural progenitor) driving Cre recombinase expression crossed with mice expressing floxed MBOAT7 exon 5. B) Of the aforementioned promoters, only Nestin-Cre driven KO produces a similar cortical lamination phenotype as straight knockout mice at E18.5. C) Ctip2+ cell numbers were not significantly different between WT and conditional knockouts, nor with straight knockouts. D) There were significantly fewer Cux1+ cells in the Nestin and straight KO conditions compared to WT ($n > 5$; $p < 0.05$).

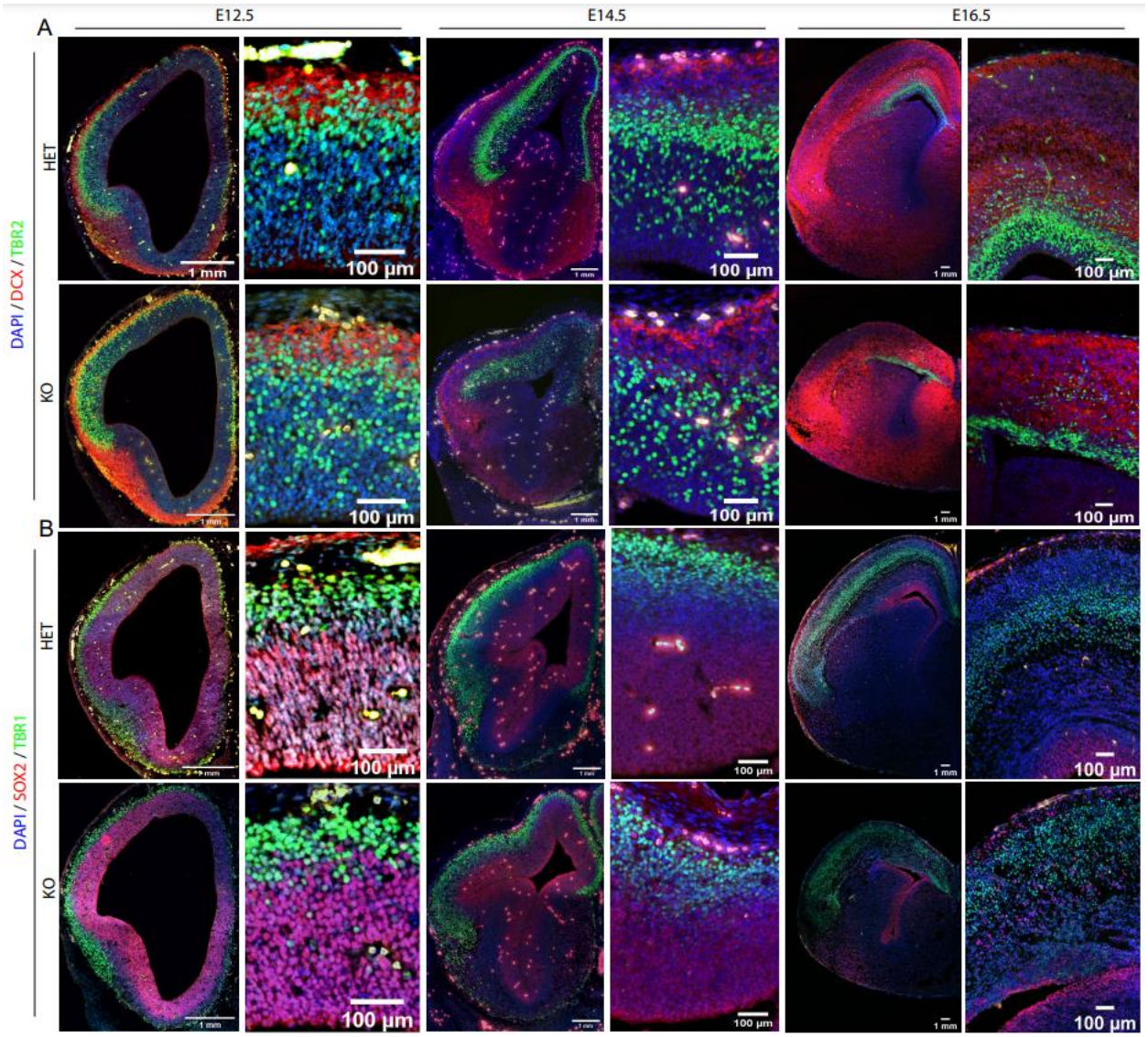

Figure 4: MBOAT7 KO leads to sequential altered radial glia patterning in the mouse cortex
A) Tbr2+ intermediate progenitors show diminished expression at E14.5 and E16.5 in homozygous MBOAT7 knockout compared to heterozygous knockout, but not E12.5. B) Tbr1+ early neurons show scattered expression at E16.5, but not E12.5 or E14.5. DCX and Sox2 expression appear similar across conditions.

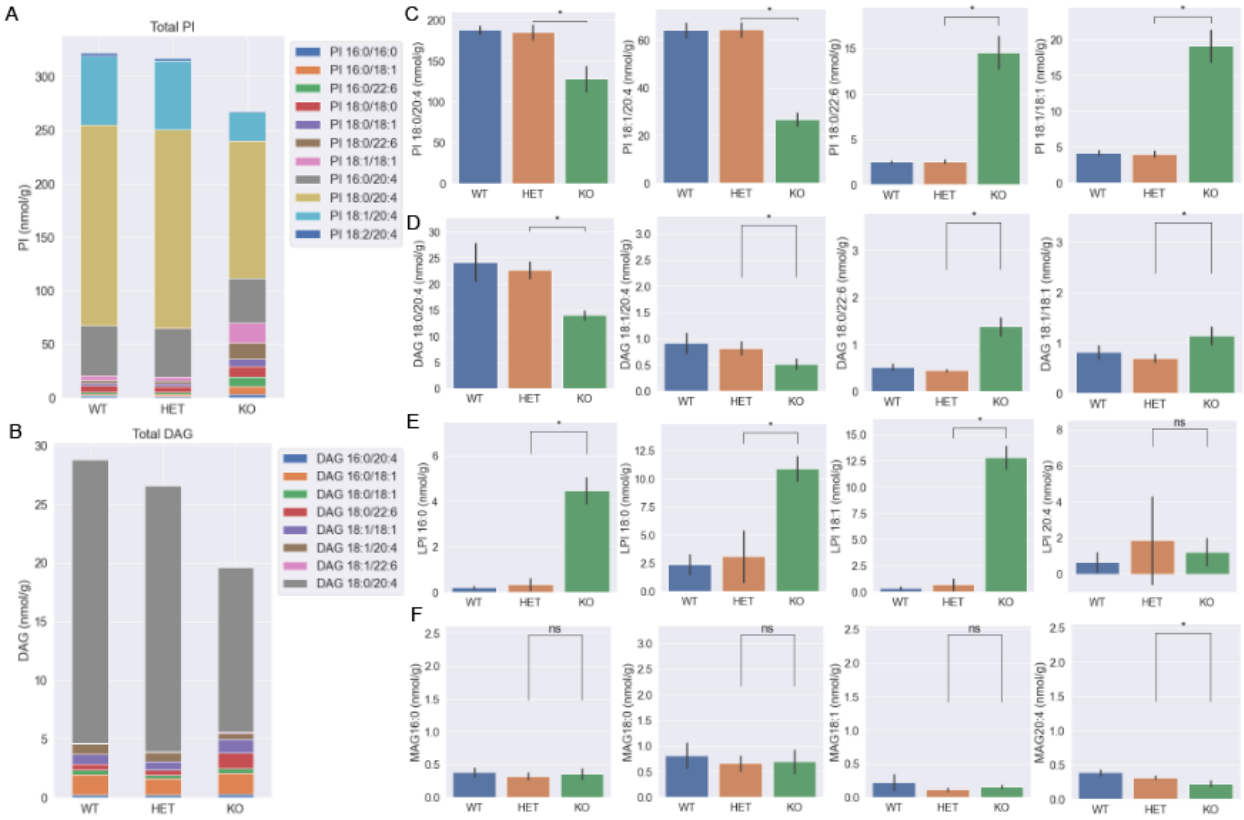

Figure 5: Lipidomics in the MBOAT7 KO brain at E13.5

A) Total PI levels are less in the E13.5 homozygous MBOAT7 KO mouse brain compared to heterozygous and WT mice. B) Total DAG levels are also lower in the KO brain, with the difference being made up mainly by the predominant 18:0/20:4 species. C) Most 20:4 containing PI species are significantly decreased in KO compared to heterozygous mice. This is accompanied by increases in all non-20:4 containing PIs. D) DAGs show similar proportions to PI, but the severity is significantly less. E) Non-20:4 containing LPIs are elevated, whereas 20:4-containing LPIs are not significantly different. F) 20:4 MAGs are slightly but significantly downregulated, but other MAG species are not. (n = 4, $p < 0.05$)

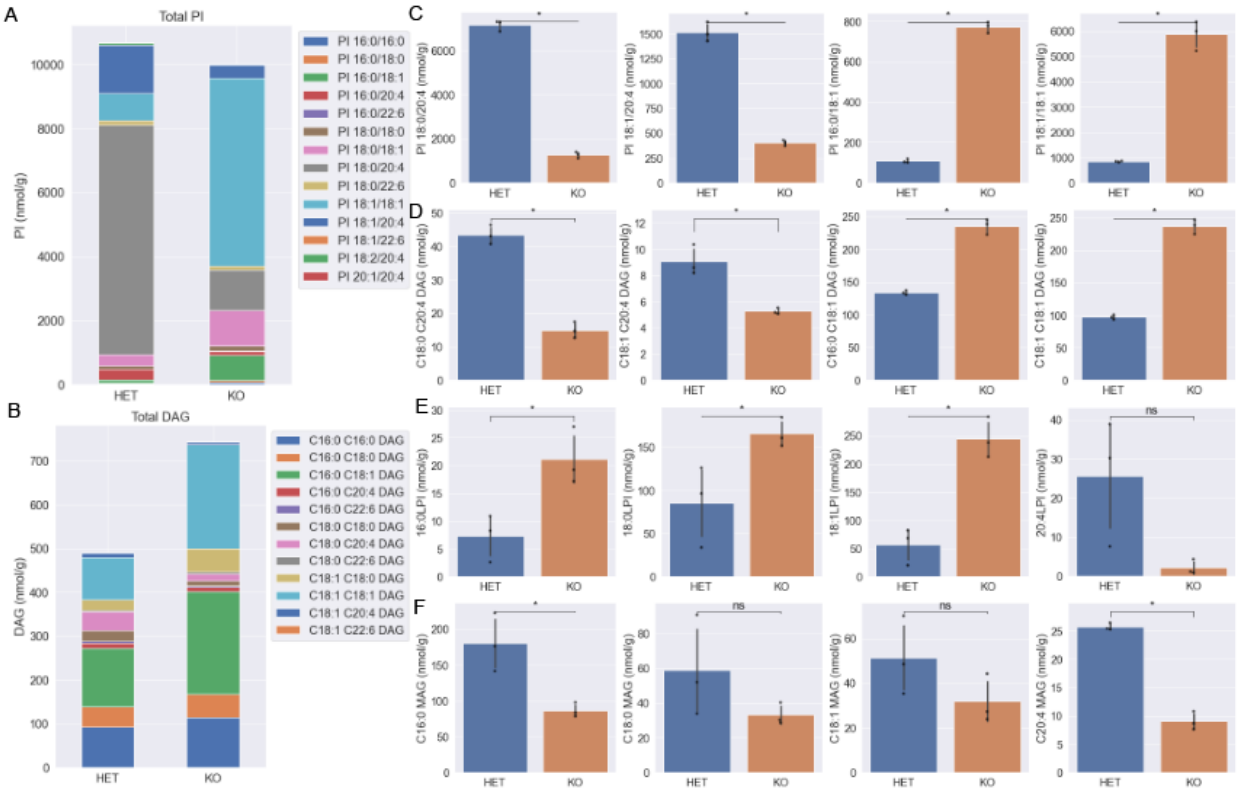

Figure 6: Lipidomics in MBOAT7 KO patient-derived NPCs

A) Similar to the E13.5 brain, total PI is slightly diminished in homozygous knockout cells compared to heterozygous cells. Making up the difference appears to be 18:1/18:1 PI Non-20:4 containing species are significantly increased. B) In contrast to the E13.5 mouse brains, total DAG seems to be higher in KO cells compared to controls. C) As seen before, 20:4-containing PI species are significantly lower, and non 20:4-containing species significantly higher. D) DAG profiles are similar to the PI profiles, but like in the mice, the differences are less severe than in PI. E) Non 20:4-containing LPI species are upregulated, but not 20:4 LPI containing species. F) Differences between MAGs in KO versus heterozygous cells seem to be slightly less, but not significantly different. ($n = 3$, $p < 0.05$)

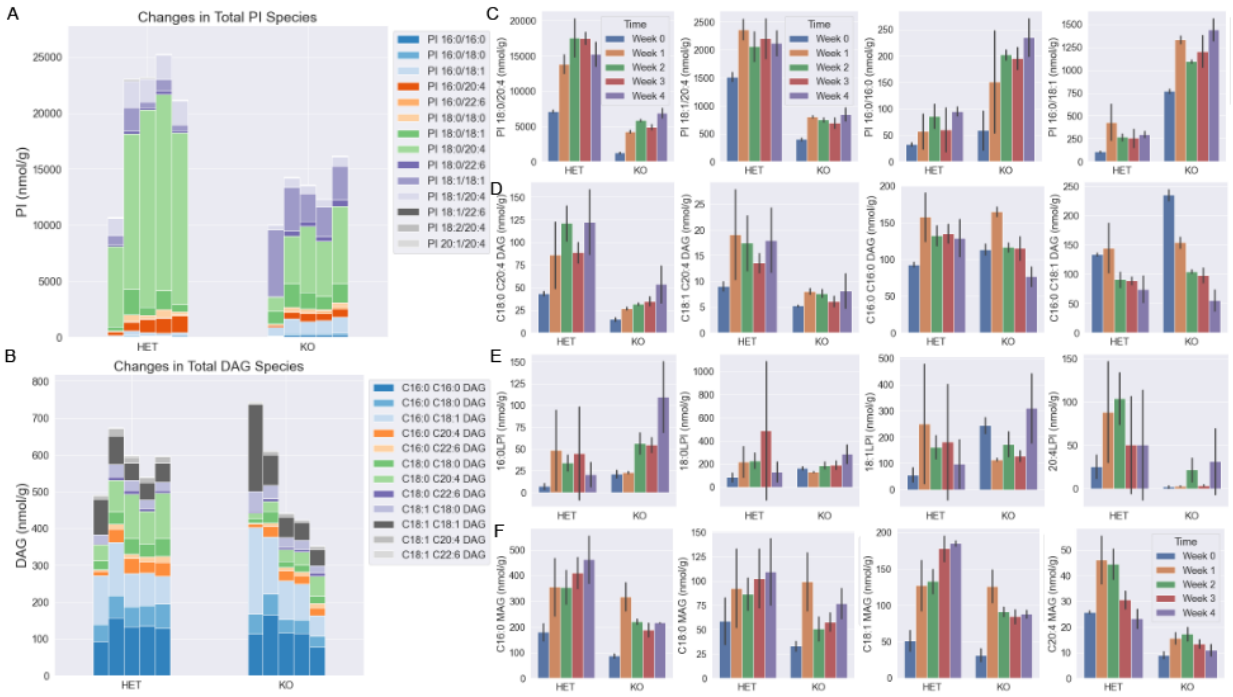

Figure 7: Differentiation reveals a dynamic lipid profile in patient NPCs
A) In general, as the NPCs differentiate overall PI levels increase in both the heterozygous and KO cells. B) DAG levels increased in the heterozygous but decreased in the KO cells as the cells differentiated. C) In some PIs, as the cells differentiated, the proportional level of PI between the heterozygous and KOs stayed the same. However, 16:0 containing PIs increased their differences between the KOs and the heterozygotes. D) Some species of DAG increased as differentiation occurred, whereas some species of DAG decreased. E) Generally, LPIs tend to increase in both conditions. F) MAG species also appeared to increase over differentiation except for the 20:4 containing with peaked at week 2 and diminished thereafter.

REFERENCES

1) Fahy, E., Cotter, D., Sud, M., & Subramaniam, S. (2011, November). *Lipid classification, structures and tools*. Biochimica et biophysica acta. https://www.ncbi.nlm.nih.gov/pmc/articles/PMC3995129/.

2) Catala, A. (2019). Introductory Chapter: Endoplasmic Reticulum-Knowledge and Perspectives. *Endoplasmic Reticulum*. https://doi.org/10.5772/intechopen.82089

3) Anderson, K. E., Kielkowska, A., Durrant, T. N., Juvin, V., Clark, J., Stephens, L. R., & Hawkins, P. T. (2013). Lysophosphatidylinositol-Acyltransferase-1 (LPIAT1) Is Required to Maintain Physiological Levels of PtdIns and PtdInsP2 in the Mouse. *PLoS ONE*, *8*(3). https://doi.org/10.1371/journal.pone.0058423

4) Wallroth, A., & Haucke, V. (2018). Phosphoinositide conversion in endocytosis and the endolysosomal system. *Journal of Biological Chemistry*, *293*(5), 1526–1535. https://doi.org/10.1074/jbc.r117.000629

5) Harayama, T., & Riezman, H. (2018). Understanding the diversity of membrane lipid composition. *Nature Reviews Molecular Cell Biology*, *19*(5), 281–296. https://doi.org/10.1038/nrm.2017.138

6) Singh, S. A., Chauhan, A., Brockerhoff, H., & Chauhan, V. P. S. (1994). Interaction of protein kinase C and phosphoinositides: regulation by polyamines. *Cellular Signalling*, *6*(3), 345–353. https://doi.org/10.1016/0898-6568(94)90039-6

7) Vance, D. (2019). Decision letter: Obesity-linked suppression of membrane-bound O-acyltransferase 7 (MBOAT7) drives non-alcoholic fatty liver disease. https://doi.org/10.7554/elife.49882.036

8) Lee, H.-C., Inoue, T., Sasaki, J., Kubo, T., Matsuda, S., Nakasaki, Y., Hattori, M., Tanaka, F., Udagawa, O., Kono, N., Itoh, T., Ogiso, H., Taguchi, R., Arita, M., Sasaki, T., & Arai, H. (2012). LPIAT1 regulates arachidonic acid content in phosphatidylinositol and is required for

cortical lamination in mice. *Molecular Biology of the Cell*, *23*(24), 4689–4700. https://doi.org/10.1091/mbc.e12-09-0673

9) Olson, E. C. (2014). Analysis of Preplate Splitting and Early Cortical Development Illuminates the Biology of Neurological Disease. *Frontiers in Pediatrics*, *2*. https://doi.org/10.3389/fped.2014.00121

10) Nakajima, S., Gotoh, M., Fukasawa, K., Murakami-Murofushi, K., & Kunugi, H. (2019). Oleic acid is a potent inducer for lipid droplet accumulation through its esterification to glycerol by diacylglycerol acyltransferase in primary cortical astrocytes. *Brain Research*, *1725*, 146484. https://doi.org/10.1016/j.brainres.2019.146484

11) Vezzani, A. (2017). Faculty Opinions recommendation of Cannabinoid receptor 1/2 double-knockout mice develop epilepsy. *Faculty Opinions – Post-Publication Peer Review of the Biomedical Literature*. https://doi.org/10.3410/f.732080065.793538857